Applied Catalysis B: Environmental 144 (2014) 107–111

Contents lists available at ScienceDirect

Applied Catalysis B: Environmental

journal homepage: www.elsevier.com/locate/apcatb

Electrochemical oxidation of dichlorvos on SnO_2—Sb_2O_5 electrodes

Ronald Vargas[a,*], Stephanie Díaz[a,b], Lucianna Viele[b], Oswaldo Núñez[b], Carlos Borrás[a], Jorge Mostany[a], Benjamín R. Scharifker[a,c]

[a] Laboratorio de Electroquímica, Departamento de Química, Universidad Simón Bolívar, Apartado 89000, Caracas 1080A, Venezuela
[b] Laboratorio de Fisicoquímica Orgánica y Química Ambiental, Departamento de Procesos y Sistemas, Universidad Simón Bolívar, Apartado 89000, Caracas, Venezuela
[c] Universidad Metropolitana, Apartado 76819, Caracas 1070A, Venezuela

ARTICLE INFO

Article history:
Received 9 February 2013
Received in revised form 13 June 2013
Accepted 18 June 2013
Available online 27 June 2013

Keywords:
Electrocatalysis
Dichlorvos (2,2-dichlorovinyl dimethyl phosphate)
Metal oxide electrode
Langmuir–Hinshelwood kinetics
Advanced oxidation process

ABSTRACT

The effects of electrode potential and the initial concentration of 2,2-dichlorovinyl dimethyl phosphate (dichlorvos, DDVP) on its oxidation/mineralization reaction kinetics, using an electrochemical oxidation system based on SnO_2—Sb_2O_5 anodes, have been studied. Electrochemical degradation followed the Langmuir–Hinshelwood mechanism, with adsorption equilibrium constant $K = 0.082\ L\ mg^{-1}$ of dichlorvos on the electrode material surface, and reaction rate constant $k = 0.021\ mg\ L^{-1}\ s^{-1}$ of the organic compound-electrocatalyst adduct. Chemical oxygen demand and CO_2 measurements in neutral media suggest that the rate limiting step for mineralization is the same as for the electrochemical oxidation. The results show that the electrochemical mineralization of dichlorvos was readily possible at potentials more positive than 2.5 V vs. SCE, with lower reaction half-lives than obtained with other advanced oxidation process. The fastest overall degradation rate constants were obtained at limiting low concentrations of dichlorvos in aqueous solution, $k_{obs} = kK = 0.0017\ s^{-1}$.

1. Introduction

2,2-Dichlorovinyl dimethyl phosphate (dichlorvos, DDVP) is an organophosphorus insecticide used in the elimination of pests affecting pear, apple, potato, tomato, cotton, onion, corn, rice and other crops. This insecticide is highly toxic to humans, mammals and aquatic animals, and few studies of its degradation through advanced oxidation processes have been reported in the literature [1]. For instance, the photodegradation of DDVP using TiO_2 and ZnO as catalyst under UV irradiation emitted by a high-pressure mercury vapor lamp, has been published [2], and the kinetics of DDVP decay under TiO_2/UV-A degradation, with considerations on the degradation mechanism, have also been reported [1,3]. Additionally, DDVP degradation using the Fenton reagent [4–6] and hydrodynamic cavitation with assisted peroxidation [7], have been evaluated as a method for water remediation from pesticide residues. The aim in these researches has been to establish the pseudo-first-order kinetic parameters of the oxidation process and the toxicity of the reaction intermediates. Thus dichlorvos is an important pollutant worth studying from practical and mechanistic reasons. Moreover, we have chosen DDVP as model pollutant for the evaluation of the electrochemical oxygen transfer reaction using an anode material with high overvoltage for water decomposition, SnO_2—Sb_2O_5.

The electrochemical oxidation of organic compounds to carbon dioxide and water on metal oxide electrodes (MO_x), occurs through complex mechanisms that involve multiple steps [8–14], including transport of the organic compound (R_{sol}) to the electrode surface (R_s),

$$R_{sol} \rightarrow R_s \quad (1)$$

followed by the establishment of an adsorption–desorption equilibrium,

$$R_s + MO_x[\ ] \overset{K}{\rightleftharpoons} MO_x[R] \quad (2)$$

and electron transfer at the electrode–electrolyte interface,

$$MO_x[R] \rightarrow MO_x[R^{\bullet +}] + e^- \quad (3)$$

In addition, under these conditions water decomposition into adsorbed hydroxyl radicals readily occurs,

$$MO_x[\ ] + H_2O \rightarrow MO_x[OH^{\bullet}] + H^+ + e^- \quad (4)$$

Free radicals formed on the electrode material surface are highly reactive and generally promote oxidation of organic substrates via hydrogen abstraction, addition to double bonds or aromatic rings [8–14].

$$MO_x[OH^{\bullet}] + MO_x[R^{\bullet +}] \rightarrow MO_x[\ ] + MO_x[P] \overset{OH^{\bullet}}{\longrightarrow} xCO_2 + yH_2O \quad (5)$$

* Corresponding author. Tel.: +58 0212 906 3968; fax: +58 0212 906 3969.
E-mail address: ronaldvargas@usb.ve (R. Vargas).

0926-3373/$ – see front matter © 2013 Elsevier B.V. All rights reserved.
http://dx.doi.org/10.1016/j.apcatb.2013.06.016

However, oxidation of organic species through oxygen transfer is invariably accompanied by oxygen evolution,

$$MO_x[OH^{\bullet}] + H_2O \rightarrow MO_x[\,] + O_2 + 3H^+ + 3e^- \quad (6)$$

Electrochemical oxygen transfer reactions have been investigated for many organic compounds on different metal oxides electrodes and have been proposed as a direct method for degradation of organics in wastewater treatment [9,12,14]. This method is able to diminish extensively the organic load and toxicity of the wastewaters; total organic carbon (TOC) and chemical oxygen demand (COD) have been used to monitor the degradation of organic matter, indicating high degradation levels [12]. In this work, dichlorvos solutions were degraded and mineralized using SnO_2—Sb_2O_5 electrodes, in order to evaluate the efficiency as compared to other methods for DDVP degradation using advanced oxidation processes. The implications of the kinetics results are also discussed.

2. Experimental

2.1. Materials

The following reactants were used without further purification: dichlorvos (2,2-dichlorovinyl dimethyl phosphate), $C_4H_7Cl_2O_4P$, 76.2%, Insecticidas Internacionales (INICA); sodium sulfate, Na_2SO_4, 99%, Aldrich; hydrochloric acid, HCl, puriss, Riedel de Haën; sodium hydroxide, NaOH, 99%, Mallinckrodt; potassium monobasic phosphoric acid, KH_2PO_4, 99%, Riedel de Haën; potassium dibasic phosphoric acid, K_2HPO_4, 98%, Riedel de Haën; sulfuric acid, H_2SO_4, 95–97%, Riedel de Haën; potassium dichromate, $K_2Cr_2O_7$, 99.5%, Merck; potassium hydrogen phthalate, $C_8H_5KO_4$, 99.5%, Riedel de Haën; water, H_2O, 17.7 MΩ cm^{-1}, Nanopure®.

Antimony-doped tin oxide (ATO), SnO_2—Sb_2O_5, thickness 1.0 μm, resistance ~70 Ω cm^{-1}, obtained from PPG industries was used as working electrode. Platinum (Pt, 99.99%), from Aldrich was the secondary electrode, and saturated calomel electrode (SCE), $Hg/Hg_2Cl_2/KCl$, E = 244 mV vs. SHE at 298 K obtained from Cole-Parmer® was the reference electrode. Information on the stability of SnO_2—Sb_2O_5 electrodes during the electrochemical oxidation of organic compounds can be obtained from the literature [12,14] and the references therein.

2.2. Dichlorvos electrochemical oxidation

Electrolyses at constant potentials were carried out with an Autolab model PGSTAT12 Potentiostat/Galvanostat under Gpes v. 4.9 Operating Software. Measurements were conducted using a three-compartment glass cell with a glass frit separating the working and secondary electrode compartments. A large area platinum gauze and a saturated calomel electrode were used as a secondary and reference electrodes respectively. Working electrodes were prepared from antimony-doped tin oxide thin films deposited on glass substrate, obtained from PPG industries with sheet resistance of ~70 Ω cm^{-1}. Electrical contacts to silver wires were realized with silver-loaded epoxy, and these assemblies were isolated with Teflon® thermally shrinkable tubing in order to expose 1.0 cm^2 of SnO_2—Sb_2O_5 geometrical surface to the solution. The electrode potential tested in the electrochemical oxidation of 15 mg L^{-1} of DDVP were 1.8, 2.0, 2.3, 2.5 and 2.7 V (vs. SCE); and at 2.5 V the DDVP initial concentration effect (4, 10, 15, 23, 35, 58, 69 and 87 mg L^{-1}) was elucidated. Reagents were of analytical grade and all solutions were prepared with distilled and ultrafiltered (Nanopure®) water, using 0.1 M Na_2SO_4 in a phosphate buffer as supporting electrolyte.

Variation of the DDVP concentration levels during electrolysis at room temperature was determined from UV–vis spectra. Spectroscopic data were obtained with a Hewlett Packard 8452A diode-array spectrometer under HP 89531 MS-DOS UV/vis Operating Software. Calibration curve according the Lambert–Beer law was previously prepared.

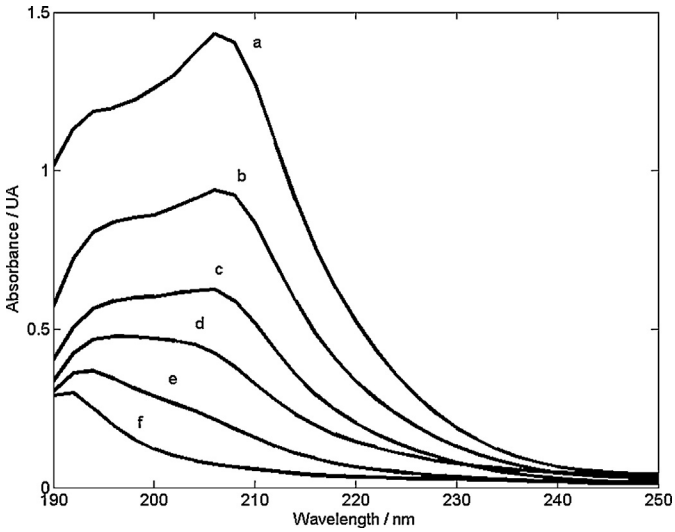

Fig. 1. UV absorption spectra of dichlorvos during electrochemical degradation. c = 15 mg L^{-1} and E = 2.5 V vs. SCE. Sample times: (a) 0, (b) 360, (c) 720, (d) 1080, (e) 1800, and (f) 5400 s.

2.3. Dichlorvos Langmuir adsorption isotherms on SnO_2—Sb_2O_5

Langmuir adsorption isotherms of DDVP on antimony-doped tin oxide were obtained at room temperature contacting a large area of the electrode material (5.3 × 10^3 cm^2), with 10 mL of solutions of the organic compound at different concentrations. This setup was stirred until the adsorption equilibrium was reached. The equilibrium concentrations of the DDVP were determined from UV–vis spectra, and the amounts of adsorbed DDVP on the metal oxide surface were calculated in each case from the difference between initial and final concentration in solution.

2.4. Chemical oxygen demand and CO_2 measurements

Organic matter diminution during electrocatalytic oxidation of DDVP was established measuring the chemical oxygen demand according to the colorimetric method [15]. For COD analysis a reaction aliquots of 3 mL were taken at different reaction times, then the organic sample content was oxidized in a closed systems using sulfuric acid and potassium dichromate for 2 h at 150 °C. The solution absorbance at 600 nm was measured. From this absorbance, the solution COD was obtained using a calibration curve made with potassium hydrogen phthalate. Mineralization was confirmed by direct CO_2 measurement using an OxyGuard portable dissolved CO_2 analyzer based on non-dispersive infrared spectrometry (NDIR).

3. Results and discussion

3.1. Kinetics of the electrochemical oxidation of dichlorvos

The degradation of many organic compounds on SnO_2—Sb_2O_5 electrodes has been studied previously [16–23], and it has been determined that efficient conversion to CO_2 occurred at electrode potentials more positive than 2.0 V respect to the saturated calomel electrode (SCE). Fig. 1 shows UV spectra during DDVP electrooxidation on SnO_2—Sb_2O_5 electrode at 2.5 V vs. SCE. The DDVP absorption band with maximum at 206 nm decreases continuously vanishing completely at sufficiently long times; this was

Table 1
Kinetic parameters during electrochemical oxidation of dichlorvos on SnO_2—Sb_2O_5 electrodes in neutral media: pseudo-first-order kinetic constant (k_{obs}), reaction half-life ($t_{1/2}$) and DDVP conversion (X_{DDVP}).

E/V vs. SCE	c_{DDVP}/mg L^{-1}	$10^4 k_{obs}$ s^{-1}	$10^{-3} t_{1/2}$ s^{-1}	X_{DDVP} (%)
1.8		3.7	1.9	82
2.0		5.8	1.2	93
2.3	15	7.3	0.95	96
2.5		7.8	0.88	97
2.7		8.2	0.85	97
	4	13	0.53	98
	10	1.0	0.72	97
	15	7.8	0.88	96
	23	6.0	1.2	94
2.5	35	4.5	1.5	91
	58	3.0	2.3	84
	69	2.7	2.6	81
	87	2.2	3.2	72

used to obtain the DDVP concentration at different times during the reaction (~90 min electrolysis for each concentration). The intermediates formed during reaction between DDVP and hydroxyl radicals have been reported [1] and do not show absorption bands in UV spectra, therefore the DDVP concentration determination using the Lambert–Beer law is a direct procedure. The main results obtained for the electro-degradation of DDVP are reported in Table 1. The pseudo-first-order kinetic constants (k_{obs}) were calculated from the slope of ln(c) vs. t plots; reaction half-lifes ($t_{1/2}$) were also estimated from the experiments, and finally, the DDVP conversions (X_{DDVP}) at 90 min of reaction under each condition are also reported. All experiments reached high DDVP conversion (70–98%). The pseudo-first-order kinetic constant increased with the electrode potential, reaching maximum value at $E > 2.5$ V vs. SCE; under this condition the hydroxyl radical coverage on the electrode surface may be estimated as a limiting value according to the mathematical model suggested in the literature [24], and then the second-order kinetic constant (k_2) for DDVP oxidation can be calculated. The obtained value ($k_2 = 2.2 \times 10^9$ M^{-1} s^{-1}) is consistent with recent theoretical computations for the reaction between hydroxyl radicals and organic compounds in homogeneous phase [25].

We also report in Table 1 the pseudo-first order kinetic constant k_{obs} values, indicating that the reaction becomes faster when the initial concentration of DDVP is lower. The effects of the initial concentration of DDVP on the slope of the ln(c) vs. t plots during the electrochemical oxidation process are shown in Fig. 2. This observation is in agreement with the Langmuir–Hinshelwood (L–H) kinetic model [26–31],

$$r = \frac{kKc}{1 + Kc} \tag{7}$$

where r (mg L^{-1} s^{-1}) is the reaction rate, c (mg L^{-1}) is the substrate concentration in water, k (mg L^{-1} s^{-1}) is the degradation rate constant at maximum coverage of the adsorbed pollutant, and K (L mg^{-1}) is the Langmuir adsorption constant of pollutant on the catalyst surface. Fig. 3 shows the reaction rate obtained during the DDVP electro-oxidation. The value of K characterizes the fraction of DDVP in the solution adjacent to the electrode surface adsorbing on the catalyst and reacting with adsorbed hydroxyl radicals, with limiting degradation rate k at maximum coverage. At low DDVP concentration, $Kc \ll 1$ and $r \approx kKc$, thus a linear increase of the rate is observed. However, at higher DDVP concentrations $Kc \gg 1$, and a limiting reaction rate $r = k$ is observed. The inset in Fig. 3 shows a linear representation of the L–H model in r^{-1} vs. c^{-1} coordinates, from which the adsorption equilibrium constant K of dichlorvos on the electrode surface and the reaction rate constant k of the organic compound-electrocatalyst adduct have been obtained

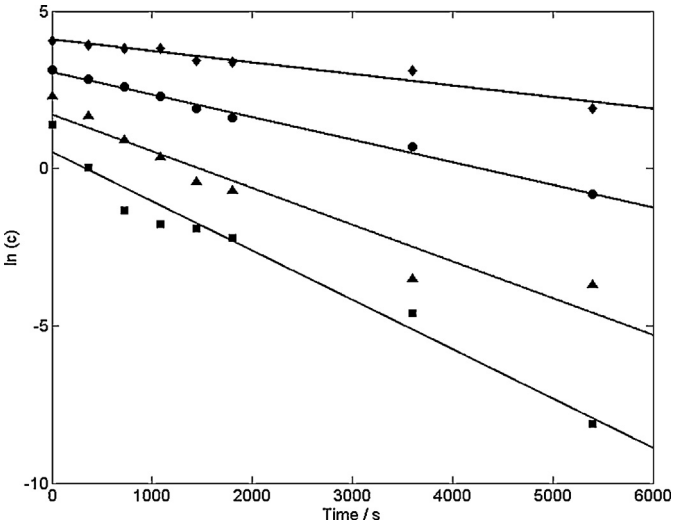

Fig. 2. Effect of the initial concentration of dichlorvos (c_0) on the slope of the ln(c) vs. time plots during the electrochemical oxidation process. c_0: (■) 4, (▲) 10, (●) 23, (♦) 58 mg L^{-1}; (—) linear fits.

experimentally. The corresponding values are $K = 0.082$ L mg^{-1} and $k = 0.021$ mg L^{-1} s^{-1}.

The pseudo-first order kinetic constants k_{obs} observed are represented as a function of the initial DDVP concentration in Fig. 4. Considering $r = k_{obs}c$, then from the L–H model (7) we can write the following equation:

$$k_{obs} = \frac{kK}{1 + Kc} \tag{8}$$

underlining that at high concentrations k_{obs} becomes inversely proportional to the pollutant concentration. At low concentrations, with $Kc \ll 1$, k_{obs} is concentration-independent and it reaches its maximum value ($k_{obs} = kK$). Therefore, knowledge of K values is quite important in order to minimize self-inhibition of the reaction rate by the pollutant and, in any case, suitable control of the initial pollutant concentration may contribute to maximize the kinetics of the degradation. For DDVP electro-oxidation on SnO_2—Sb_2O_5 electrodes at potentials more positive than 2.5 V vs. SCE, the fastest

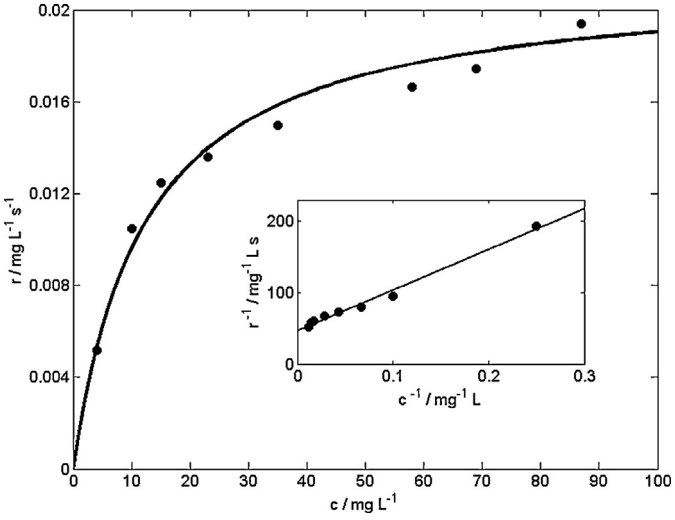

Fig. 3. Langmuir–Hinshelwood kinetics for the electrochemical oxidation/mineralization of dichlorvos at $E = 2.5$ V vs. SCE. Inset: L–H linear representation. (—) Graphical representation of the L–H Eq. (7) with $k = 2.1 \times 10^{-2}$ mg L^{-1} s^{-1} and $K = 8.2 \times 10^{-2}$ L mg^{-1}.

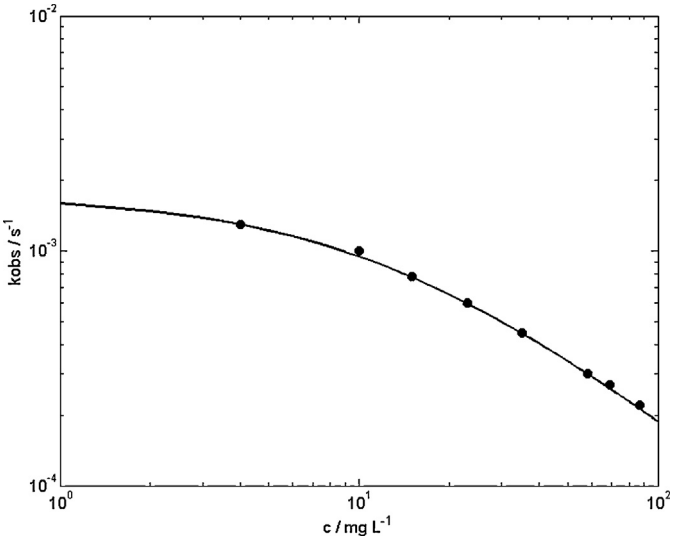

Fig. 4. Plot of k_{obs} values vs. dichlorvos initial concentrations. (—) Graphical representation of Eq. (8) with $k = 2.1 \times 10^{-2}$ mg L^{-1} s^{-1} and $K = 8.2 \times 10^{-2}$ L mg^{-1}.

degradation rate calculated using the L–H parameter (k and K) is: $k_{obs} = kK = 0.0017\ s^{-1}$.

3.2. Electrochemical mineralization of dichlorvos

Mineralization was confirmed by the measurement of the CO_2 produced during the DDVP oxidation. Fig. 5 shows that both the CO_2 formed and the COD diminution during the electrocatalytic oxidation of the DDVP, follow a kinetic model according to a consecutive reaction scheme where there are no accumulation of intermediates. Additionally, the final concentration of dissolved carbon dioxide, $CO_2(t_f)$, corresponds very well with the predicted stoichiometrically assuming that all DDVP was oxidized completely. From the slope $\ln(COD/COD_0)$ vs. time representation, a pseudo-first-order rate constant $k_{obs}^{mine} = 8.8 \times 10^{-4}\ s^{-1}$ was obtained. Under the same conditions, the DDVP electro-oxidation constant found from spectrophotometric measurements was $k_{obs} = 7.8 \times 10^{-4}\ s^{-1}$. The proximity of both values indicates that mineralization and electrochemical degradation concur under the same rate limiting step, and that there is not accumulation of intermediates during DDVP

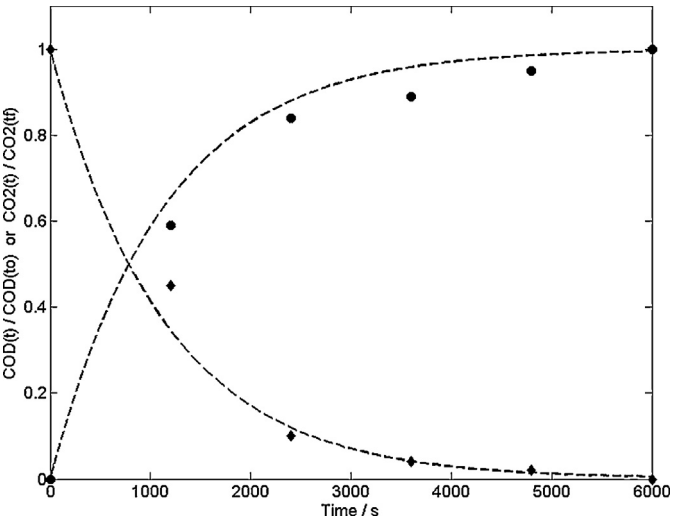

Fig. 5. CO_2 produced (●) and COD diminution (♦)during the electrocatalytic oxidation of the DDVP on SnO_2—Sb_2O_5 at 2.5 V vs. SCE. $c_0 = 15$ mg L^{-1}.

treatment under the conditions described. This is relevant, since it has been reported that toxic intermediates are formed when UV light is used to degrade DDVP in the presence of TiO_2 [2]. From these results, the reaction scheme in the presence of hydroxyl radicals adsorbed on antimony-doped tin oxide surfaces can be expressed as:

$$R_s + MO_x[\ ] \overset{K}{\rightleftharpoons} MO_x[R] \xrightarrow{k} xCO_2 + yH_2O \quad (9)$$

with $k_{obs} = k_{obs}^{mine} = kK/(1 + Kc)$.

3.3. Comparison with other heterogeneous advanced oxidation methods

The DDVP degradation values obtained for L–H parameters (k and K) using SnO_2—Sb_2O_5 at neutral pH are compared with other heterogeneous advanced oxidation process (TiO_2/UV and ZnO/UV). In the analysis of this type of heterogeneous reactions (reaction between adsorbed organic compound and adsorbed OH$^\bullet$ radicals on the catalyst surface), the reaction rate comprises a thermodynamic contribution (K) due to the interaction of the organic with the surface, and a kinetic contribution (k) due to reaction of hydroxyl radicals with adsorbed pollutant. For instance, the k values obtained for electrochemical oxidation and for ZnO/UV [2] and TiO_2/UV [2,3] degradation are the same (the values were corrected by the respective concentration of the catalyst), and correspond with the surface reactions between the DDVP and the hydroxyl radical. The equilibrium adsorption constant values depend on the interaction between the organic compound and the catalyst, and it has been found from the values obtained from the electro-oxidation data, that the interaction DDVP with SnO_2—Sb_2O_5 is much stronger than that for the other systems (TiO_2 and ZnO). Moreover, the Langmuir adsorption isotherm study without application of electrode potential reveals an adsorption–desorption constant value comparable with that obtained during the electrocatalytic oxidation. This implies that the reaction kinetics for DDVP electrochemical oxidation/mineralization is higher in comparison with other advanced oxidation methods reported so far in the literature [2,3]. In fact under this condition the fastest degradation rate for DDVP degradation on SnO_2—Sb_2O_5 anodes is obtained ($k_{obs} = kK = 0.0017\ s^{-1}$).

4. Conclusions

Electrochemical oxidation/mineralization of the insecticide dichlorvos occurs readily at neutral media on antimony-doped tin oxide at potentials higher than 2.5 V vs. SCE. A dependency of the pseudo first order rate constant (k_{obs}) values on the initial concentration of organic compound is observed owing to decomposition following the Langmuir–Hinshelwood kinetic model. In this reaction, the adsorption equilibrium constant on the electrocatalyst is relatively large, thus determining a rate constant with an inverse concentration dependence according to $k_{obs} = kK/(1 + Kc)$.

Acknowledgement

We are grateful to Lic. Estrella Vargas from Universidad Central de Venezuela for discussions.

References

[1] T. Oncescu, M.I. Stefan, P. Oancea, Environmental Science and Pollution Research 17 (2010) 1158–1166.
[2] E. Evgenidou, K. Fytianos, I. Poulios, Applied Catalysis B: Environmental 59 (2005) 81–89.
[3] P. Oancea, T. Oncescu, Journal of Photochemistry and Photobiology A: Chemistry 199 (2008) 8–13.
[4] M-C. Lu, J-N. Chen, C-P. Chang, Chemosphere 35 (1997) 2285–2293.

[5] M-C. Lu, J-N. Chen, C-P. Chang, Journal of Hazardous Materials 65 (1999) 277–288.
[6] J. Schramm, I. Hua, Water Research 35 (2001) 665–674.
[7] R.K. Joshi, P.R. Gogate, Ultrasonics Sonochemistry 19 (2012) 532–539.
[8] W.R. LaCourse, Y-H. Hsiao, D.C. Johnson, Journal of the Electrochemical Society 136 (1989) 3714–3719.
[9] Ch. Comninellis, Electrochimica Acta 39 (1994) 1857–1862.
[10] D.C. Johnson, J. Feng, L.L. Houk, Electrochimica Acta 42 (2000) 323–330.
[11] A. Kapałka, G. Fóti, Ch. Comninellis, Journal of Applied Electrochemistry 38 (2008) 7–16.
[12] M. Panizza, G. Cerisola, Chemical Reviews 109 (2009) 6541–6569.
[13] R. Vargas, C. Borrás, D. Plana, J. Mostany, B.R. Scharifker, Electrochimica Acta 55 (2010) 6501–6506.
[14] R. Vargas, C. Borrás, J. Mostany, B.R. Scharifker, Boletín de la Academia de Ciencias Físicas Matemáticas y Naturales 71 (2011) 37–56.
[15] A.L. Greenberg, A.E. Clesceri, Standard Methods for the Examination of Water and Wastewater, 18th ed., American Water Works association, Waste Environmental Federation, USA, 1992, 2-38/2-42.
[16] R. Kötz, S. Stucki, B. Carcer, Journal of Applied Electrochemistry 21 (1991) 14–20.
[17] S. Stucki, R. Kötz, B. Carcer, W. Suter, Journal of Applied Electrochemistry 21 (1991) 99–104.
[18] C. Borrás, C. Berzoy, J. Mostany, B.R. Scharifker, Journal of Applied Electrochemistry 36 (2006) 433–439.
[19] M. Tian, L. Bakovic, A. Chen, Electrochimica Acta 52 (2007) 6517–6524.
[20] C. Borrás, C. Berzoy, J. Mostany, J.C. Herrera, B.R. Scharifker, Applied Catalysis B: Environmental 72 (2007) 98–104.
[21] B. Adams, M. Tian, A. Chen, Electrochimica Acta 54 (2009) 1491–1498.
[22] R. Vargas, C. Borrás, J. Mostany, B.R. Scharifker, Water Research 44 (2010) 911–917.
[23] L. Ciríaco, D. Santos, M.J. Pacheco, A. Lopes, Journal of Applied Electrochemistry 41 (2011) 577–587.
[24] A. Kapałka, G. Fóti, Ch. Comninellis, Electrochimica Acta 54 (2009) 2018–2023.
[25] D. Minakata, K. Li, P. Westerhoff, J. Crittenden, Environmental Science and Technology 43 (2009) 6220.
[26] R.W. Matthews, Journal of Physical Chemistry 91 (1987) 3328–3333.
[27] M.R. Hoffman, S.T. Martin, W. Choi, D.W. Bahnemann, Chemical Reviews 95 (1995) 69–96.
[28] R.J. Baxter, P. Hu, Journal of Chemical Physics 116 (2002) 4379–4381.
[29] I. Kuehr, O. Núñez, Pest Management Science 63 (2007) 491–494.
[30] G. Pardo, R. Vargas, O. Núñez, Journal of Physical Organic Chemistry 21 (2008) 1072–1078.
[31] R. Vargas, C. Borrás, J. Mostany, B.R. Scharifker, Electrochimica Acta 80 (2012) 326–333.